Amino Acids (2009) 37:653–664
DOI 10.1007/s00726-008-0185-8

ORIGINAL ARTICLE

D-Aspartate affects secretory activity in rat Harderian gland: molecular mechanism and functional significance

Rossella Monteforte · Alessandra Santillo · Marcello Di Giovanni · Antimo D'Aniello · Antimo Di Maro · Gabriella Chieffi Baccari

Received: 26 June 2008 / Accepted: 17 September 2008 / Published online: 27 September 2008

Abstract In this paper, the role of D-aspartate in the rat Harderian gland (HG) was investigated by histochemical, ultrastructural, and biochemical analyses. In this gland, substantial amounts of endogenous D-Asp were detected, along with aspartate racemases that convert D-Asp to L-Asp and vice versa. We found that the gland was capable of uptaking and accumulating exogenously administered D-Asp. D-Asp acute treatment markedly increased lipid and porphyrin secretion and induced a powerful hyperaemia in inter-acinar interstitial tissue. Since D-Asp is known to be recognized by NMDA receptors, the expression of such receptors in rat HG led us to the hypothesis that D-Asp acute treatment induced the activation of the extracellular signal-regulated protein kinase (ERK) and nitric oxide synthase (NOS) pathways mediated by NMDA. Interestingly, as a result of enhanced oxidative stress due to increased porphyrin secretion, the revealed activation of the stress-activated protein kinase/c-jun N-terminal kinase (SAPK/JNK) pro-apoptotic pathway was probably triggered by the gland itself to preserve its cellular integrity.

Keywords Harderian gland · D-Aspartate · D-Amino acids · Exocrine gland

R. Monteforte · A. Santillo · M. Di Giovanni · A. Di Maro · G. Chieffi Baccari (✉)
Dipartimento di Scienze della Vita,
Seconda Università degli Studi di Napoli,
via Vivaldi, 43-81100 Caserta, Italy
e-mail: gabriella.chieffi@unina2.it

A. D'Aniello
Stazione Zoologica "A. Dohrn",
villa Comunale, Naples, Italy

List of abbreviations

AB/PAS	Alcian blue-PAS
D-Asp	D-Aspartate
ERK	Extracellular signal-regulated protein kinase
HG	Harderian gland
L-Asp	L-Aspartate
MAP	Mitogen-activated protein
NMDA	*N*-methyl-D-aspartic acid
NO	Nitric oxide
NOS	Nitric oxide synthase
SAPK/JNK	Stress-activated protein kinase/c-jun N-terminal kinase
TBS/T	Tris-buffered saline/Tween

Introduction

Free D-aspartate (D-Asp) is present in a wide variety of tissues and cells, particularly in the central nervous system and endocrine tissues (see for review, D'Aniello 2007). Because the levels of D-Asp change in a variety of organs during development, it has been suggested that it may play a significant role in regulating developmental processes (Dunlop et al. 1986; Neidle and Dunlop 1990; Wolosker et al. 2000). Although D-Asp is not metabolized by the common enzymatic systems involved in the catabolism of L-amino acids, it is nonetheless recognized by *N*-methyl-D-aspartic acid (NMDA) receptors (Skerritt and Johnston 1981; Foster and Fagg 1987, Nahm et al. 2004). Thus, important biological roles have been postulated for D-Asp. For instance, besides its well known neuroexcitatory activity, D-Asp is crucial for neurotransmission and neurosecretion in the central nervous system, as well as for the biosynthesis and/or secretion of hormones in endocrine

glands (Schell et al. 1997; Nagata et al. 1999; D'Aniello et al. 2000a, b; Wang et al. 2000; Wolosker et al. 2000; D'Aniello et al. 2003). However, in spite of the insightful research available on the role of D-Asp in the nervous and endocrine systems, evidence on the natural occurrence and role of this amino acid in exocrine glands is still lacking. High concentrations of D-Asp have been found in the parotid and submandibular glands of 4- to 7-week-old rats (Masuda et al. 2003). Recently, we have demonstrated that high concentrations of free D-Asp modulate secretion in the Harderian glands (HGs) of the frog *Rana esculenta* (Raucci et al. 2005), and lizard *Podarcis s. sicula* (Santillo et al. 2006). The Harderian gland is an orbital gland found in the majority of land vertebrates (see for reviews Payne 1994; Chieffi et al. 1996). One of its main characteristics is its extreme morphological and biochemical variability among species, a peculiarity that for the most part reflects its versatile functional role in environmental adaptation. For instance, in amphibia and reptiles HG produces serous-mucous secretion (see for reviews Payne 1994; Chieffi et al. 1996); in rodents it secretes prevalently lipoproteins (Seyama et al. 1992), porphyrins (Gorchein 2003), as well as low amounts of serotonin (Djeridane et al. 1999) and melatonin (Djeridane et al. 1998; Coto-Montes et al. 2003). Although its main role is to lubricate the eye, rodent HG may be a source of pheromones and growth factors (Seyama et al. 1992) and may be implicated in photoreception (Hugo et al. 1987), in thermoregulation (Thiessen 1988; Shanas and Terkel 1996), or in the retinal-pineal axis (Hoffman et al. 1989).

In the present study, we demonstrated that substantial amounts of free D-Asp are present in the HG of rats. To gain insight into the functional significance of D-Asp in HG, we administered D-Asp i.p. to adult rats and then investigated its effects on HG secretory activity by histochemical, ultrastructural and biochemical analyses. We found that the gland possesses the capability to uptake and accumulate D-Asp when exogenously administered. Further, we found an enhanced gland secretion as well as a powerful hyperaemia in rat HG-D-Asp treated. Furthermore, since D-Asp is recognized by receptors for NMDA (Skerritt and Johnston 1981; Foster and Fagg 1987), we determined the presence of NMDA receptors in rat HG by RT-PCR so as to establish the potential molecular pathways elicited by the activation of NMDA receptors-D-Asp mediated.

Materials and methods

Animals

Male Wistar rats, *Rattus norvegicus albinus,* weighing 200–250 g, were housed under regulated conditions of temperature (28°C) and light (12 h:12 h L:D cycles). They received commercial food pellets (Mil-Rat, Morini, Italy) and water ad libitum.

Experiments

Rats ($N = 30$) were injected i.p. with 2.0 μmol/g D-aspartate (D-Asp) (Sigma, Milan, Italy) dissolved in saline solution. The dose was chosen on the basis of preliminary experiments carried out with different doses (0.5–4.0 μmol/g body weight) of D-Asp. Control rats ($N = 6$) received saline injection. At different time points (15 min, 30 min, 45 min, 1 h, 2 h, 6 h) after the amino acid injection, the animals were anesthetized by an i.p. injection of chloral hydrate (40 mg/g body mass) and then decapitated. After dissecting the Harderian glands, we weighed and rapidly immersed one gland from each animal in fixative for light or electron microscopy. The contralateral glands were immediately stored at −20°C for biochemical analyses. The liver and brain were dissected in the same way as the control tissues. The experiment was repeated twice. The experimental protocol, as well as the housing conditions, was in accordance with the Italian guidelines (D.Lvo 116/92) and authorized by the local Animal Care Committee (Servizio veterinario ASL 44, Prot. Vet. 22/95).

Amino acid analysis

Harderian glands and livers from each animal were first homogenized (Ultra-Turrax T25 homogenizer) with 0.1 M trichloroacetic acid (TCA) in a ratio of 1:10 and then centrifuged at 15,000*g* for 10 min. The supernatants were neutralized (at pH 6–8) using 1 M NaOH. To determine the presence of D- and L-amino acids, the resulting samples were purified. Next, HPLC determination was performed (Raucci et al. 2005).

Determination of racemases: D-Asp → L-Asp and L-Asp → D-Asp

The determination of racemase activity was carried out using a radioactive method based on the use of [^{14}C]D-Asp or [^{14}C]L-Asp, according to a modified procedure described by Wolosker et al. (2000). Briefly, to determine the racemase activity that converts L-Asp to D-Asp (L-Asp → D-Asp racemase), 100 mg of rat HG was homogenized in 800 μl of Krebs–Ringer solution (NaCl 110 mM, KCl 4.6 mM, $CaCl_2$ 10 mM, $MgCl_2$ 6.6 mM, $NaHCO_3$ 25 mM, NaH_2PO_4 14 mM, glucose 15 mM, and HEPES 10 mM, which was adjusted to pH 7.5 with some drops of 1 M NaOH) containing a cocktail of protease inhibitors (Sigma Chemical Company, code P 8340). The mixture was centrifuged for 20 min at 13,000*g* and the supernatant dialyzed

against Krebs–Ringer solution at 4°C. This procedure ensures the elimination of endogenous amino acids present in the tissue homogenates. Then, 1 ml of the dialyzed sample (pH 7.5) was mixed with 2.0 µl of [^{14}C]L-Asp 1 µCi/ml (0.05 pmol/ml) and incubated at 37°C. After 1, 2 and 4 h, 200 µl of sample (20 mg tissues; 880,000 CPM) was mixed with 5 µl of 4 M TCA to block the reaction. Then, it was centrifuged at 12,000*g* for 5 min. Next, 100 µl of the supernatant was mixed with 10 µl of 1 M NaOH (to neutralize the TCA), 83 µl of 0.05 M pyrophosphate buffer, pH 10, 1.0 µl of cold D-Asp (10 nmol/ml), 1.0 µl of cold (L-Asp 10 nmol/ml) and 5 µl of OPA-NAC. After 2 min, 100 µl of this mixture was injected into the HPLC column (Supelcosil C-18 HPLC column, 0.45 × 25 cm, 5 µm beads, Supelco, USA) to separate D-Asp from L-Asp (Raucci et al. 2005). Since the labeled D-Asp and L-Asp are undetectable by the HPLC, a defined amount of cold D-Asp and L-Asp was added to the sample in order to visualize and to collect the peaks of these amino acids during the HPLC run.

To determine the racemase activity that converts D-Asp to L-Asp (D-Asp → L-Asp racemase), we adopted the same procedure with the same homogenized and dialyzed samples, but with 2.0 µl of [^{14}C]D-Asp 1 µCi/ml (0.1 pmol) instead of [^{14}C]L-Asp. The racemase activities were also assayed at pH 5.5 (0.05 M citrate-phoshate buffer) and at pH 8.5 (tris–HCl 0.05 M).

Histology, histochemistry and ultrastructure

Harderian glands were rapidly immersed in Bouin's fluid; then, paraffin sections (5-µm thick) were cut and stained with Mallory's trichrome stain. Mucosubstances were detected with Alcian blu/PAS (AB/PAS) technique, whereas proteins were determined with the mercury bromophenol blue method. For lipid detection, formol-calcium-fixed frozen sections (5–10 µm) were stained with Sudan Black B.

For electron microscopy, samples of HG (3 mm^3) were first promptly immersed for 2 h in Karnovsky's fixative in cacodylate buffer (pH 7.4) and then post-fixed for 1 h in Millonig's buffer containing 1% osmium tetroxide. The samples were dehydrated through a graded ethanol series and finally embedded in Epon 812. Ultra-thin sections, first stained with 4% uranyl acetate and then with 1% lead citrate, were examined with the Zeiss LEO-912 transmission electron microscope (Zeiss, Germany).

Porphyrin detection

Total porphyrin concentration was measured by fluorescence spectroscopy (Buzzell et al. 1989). HGs were weighed and homogenized (Ultra-Turrax T25 homogenizer) in 5 ml of an organic phase consisting of ethyl acetate:acetic acid (8:2). Following centrifugation, 50 µl portions were extracted in 1.5 N HCl. Fluorescence was read in a Perkin-Elmer LS50B fluorescence spectrophotometer at an excitation wavelength of 405 nm and at an emission wavelength of 604 nm. Samples were compared with standards made of coproporphyrin III tetramethyl ester. Porphyrin concentrations were expressed as µg/mg tissue.

RNA isolation and RT-PCR of NMDA receptors (NR-1, NR-2)

Total RNA was isolated from both Harderian gland and brain using TRIzol Reagent (Life Technologies, Gaithersburg, MD) according to the protocol supplied by the manufacturer. The quality of the RNA samples was checked on a denaturating formaldehyde agarose gel.

Two micrograms of total RNA was reverse-transcribed using the SuperScript^{TM} First-Strand Synthesis System for RT-PCR kit (code 11904-018, Invitrogen, CA). The cDNA was added to a mix containing 5 U/µL *Taq* DNA Polymerase, 2.5 mM dNTPs, PCR buffer (all from Invitrogen, CA), and 25 µM of the relevant oligonucleotide primers (Sigma-Genosys, UK). These primers had the following sequences: NR1 sense, 5′-AATGACCCCAGGCTCAGA AAC-3′ and NR1 antisense, 5′-TGAAGCCTCAAACTCC AGCAC-3′ (GenBank accession no. U08261); NR2A sense, 5′-TATAGAGGGTAAATGTTGGA-3′ and NR2A antisense, 5′- AGAAACTGTGAGGCATTTCT-3′ (GenBank accession no. AF001423); NR2B sense, 5′-ACTGTG ACAACCCACCCTTC-3′ and NR2B antisense, 5′-CGG AACTGGTCCAGGTAGAA-3′ (GenBank accession no. U11419); NR2C sense, 5′-TGTGTCAGGCCTTAGTGA CA-3′ and NR2C antisense, 5′-CCACACTGTCTCCAGC TTCT-3′ (GenBank accession no. 08259); NR2D sense, 5′-AAGAAGATCGATGGCGTCTG-3′ and NR2D antisense, 5′-GGATTTCCCAATGGTGAAGG-3′ (GenBank accession no. L31612). As an internal control, the same cDNAs were amplified using β-actin oligonucleotide primers with the following sequences: β-actin sense, 5′-TTGTAACCAACTGGGACGATATGG-3′ and β-actin antisense, 5′-GATCTTGATCTTCATGGTGCTAGG-3′ (GenBank accession no. J00691). For the actual analysis, samples were heated for 5 min at 95°C. Then 35 cycles were carried out, each consisting of 1 min at 94°C, 1 min at 63°C, and 1.5 min at 72°C. This was followed by a final 5 min extension at 72°C. Finally, the PCR reaction products, separated on a 2% agarose gel containing EtBr, were rapidly visualized.

Protein-extract preparations

Rat Harderian glands and livers were homogenized directly in lysis buffer containing 50 mM HEPES, 150 mM NaCl,

1 mM EDTA, 1 mM EGTA, 10% glycerol, 1% Triton-X-100 (1:2 weight/volume), 1 mM phenylmethylsulphonyl fluoride (PMSF) 1 μg aprotinin, 0.5 mM sodium orthovanadate, and 20 mM sodium pyrophosphate, (Sigma Chemical Corporation, St. Louis, MO). They were then clarified by centrifugation at 14,000*g* for 10 min. Protein concentrations were estimated using a modified Bradford assay (Bio-Rad, Melville, NY).

Western blot analysis

Fifty micrograms of total protein extracts was boiled in Laemmli buffer for 5 min before electrophoresis. The samples were subjected to SDS-PAGE (10% polyacrylamide) under reducing conditions. After electrophoresis, proteins were transferred onto a nitrocellulose membrane (Immobilon Millipore Corporation, Bedford, MA). The complete transfer was assessed using prestained protein standards (Bio-Rad, Melville, NY). The membranes were first treated for 1 h with blocking solution (5% non-fat powdered milk in 25 mM Tris, pH 7.4; 200 mM NaCl; 0.5% Triton x-100, TBS/T) and then incubated over night at 4°C with the following polyclonal primary antibodies (all purchased from Cell Signaling Technology, Inc., Danvers MA, USA): (1) against phospho-ERK1/2 (Thr202/Tyr204) diluted 1:2,000; (2) against ERK1/2, diluted 1:2,000; (5) against phospho-SAPK/JNK (Thr183/Tyr185), diluted 1:1000; (6) against SAPK/JNK, diluted 1:1,000. After washing with TBS/T and TBS, membranes were incubated with the horseradish-peroxidase-conjugated secondary antibody (1:4,000) for 1 h at room temperature. The reactions were detected using an enhanced chemiluminescence (ECL) system (Amersham Life Science, UK).

Nitric oxide synthase assay

Rat HGs and livers were homogenized in PBS, pH 7.4, and centrifuged at 10,000*g* for 20 min. The supernatant was first ultracentrifuged at 1,00,000g for 15 min and subsequently filtered through a 0.45-μm filter. Forty microliters of the filtrate was used to assay nitric oxide synthase (NOS) activity using a colorimetric kit (Calbiochem, Darmstadt, Germany). The enzyme activity was expressed as nitrite + nitrate concentration (μM).

cAMP and cGMP assays

Levels of cAMP and cGMP in HGs and livers were measured with [^{3}H]cAMP assay and [^{3}H]cGMP assay kits, respectively (Amersham, NJ, USA). Briefly, HGs and livers from each animal were first homogenized with 0.1 M HCl in a ratio of 1:10, using an Ultra-Turrax T25 homogenizer, and then centrifuged for 10 min at 12,000g. The supernatants were neutralized (at pH 7.5) using 1 M NaOH and the resulting sample was used for the assays. The amount of cAMP and cGMP (pmol/g tissue) was estimated by comparing the radioactivity for each sample with that of known standards.

Statistical analyses

All data were compared using an analysis of variance (ANOVA), followed either by Duncan's test for multi-group comparisons or by a Student *t* test for between-group comparisons. All data were expressed as mean ± standard deviation. The levels of significance were set at $P < 0.001$ and $P < 0.0001$.

Results

Endogenous occurrence of D-Asp and L-Asp in rat HG in response to acute D-Asp treatment

A specific and sensitive HPLC method, entailing the diasteromeric separation of D-Asp from the other amino acids by means of a D-aspartate oxidase, revealed the endogenous occurrence of D-Asp and L-Asp in both rat HG and liver (Fig. 1). In rat HGs, the endogenous values of D-Asp (0.19 ± 0.02 μmol/g tissue) were lower than those of L-Asp (0.34 ± 0.05 μmol/g tissue). However, 30 min (1.62 ± 0.17 μmol/g tissue), 1 h (1.91 ± 0.24 μmol/g tissue), 2 h (2.63 ± 0.34 μmol/g tissue), and 6 h (3.58 ± 0.31 μmol/g tissue) after D-Asp i.p. injection, D-Asp values in the HG were significantly ($P < 0.001$) higher than those of basal values (Fig. 1). Harderian gland L-Asp levels were significantly ($P < 0.001$) higher than those of basal values at 1 h (0.89 ± 0.09 μmol/g tissue), 2 h (1.12 ± 0.13 μmol/g tissue), and 6 h (1.90 ± 0.16 μmol/g tissue)

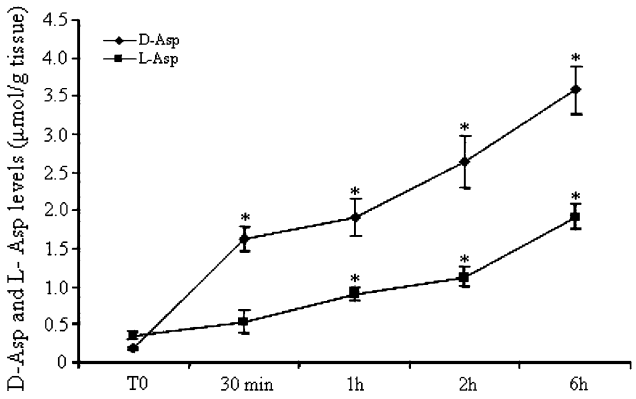

Fig. 1 Endogenous occurrence of free *D-Asp* and *L-Asp* in rat HG and their accumulation in response to *D-Asp* injection (2.0 μmol/g). The results represent the mean ± SD obtained from five individual determinations. * $P < 0.001$ versus control

after D-Asp injection (Fig. 1). Further, when D-Asp was administered, it accumulated in the rat liver, as previously reported (D'Aniello et al. 2000a). After 30 min (0.63 ± 0.07 μmol/g tissue) and 1 h (0.97 ± 0.05 μmol/g tissue) from D-Asp treatment, the levels of D-Asp were significantly higher than those of control HG (0.27 ± 0.02 μmol/g tissue). At 2 h (0.42 ± 0.04 μmol/g tissue) and 6 h (0.33 ± 0.02 μmol/g tissue) after D-Asp injection, D-Asp levels in the liver were close to control values, whereas L-Asp levels (1.21 ± 0.17 μmol/g tissue) remained unchanged.

Racemase activity in rat HG

To determine whether D-Asp is biosynthesized from L-Asp and/or whether the conversion of D-Asp to L-Asp occurs via an aspartate racemase, we measured racemase activity by evaluating the in vitro conversion of D-Asp to L-Asp and L-Asp to D-Asp. An enzymatic assay [^{14}C] with D-Asp as substrate yielded 30% of total [^{14}C]D-Asp converted to [^{14}C]L-Asp (66,000 CPM, 1.5 fmoles L-Asp) after 4 h of incubation at 37°C (Fig. 2a). Conversely, when [^{14}C]L-Asp was used as substrate, only 10% of this amino acid was converted to [^{14}C]D-Asp (22,000 CPM, 0.5 fmoles D-Asp) (Fig. 2b). Both racemase activities increased proportionally with the progress of incubation time. The maximum enzymatic activity occurred at 7.5 pH. At pH 5.5 and pH 8.5, however, the enzymatic activity was reduced by about 70% (Fig. 2c).

Morphological effects of D-Asp administration on rat HG

Histology and histochemistry

The Harderian glands of rats consist of tubule-alveolar units that are separated by connective strands (Fig. 3a). The glandular cells of the control HG contained homogeneous pale secretory vacuoles and nuclei basally located. The acinar lumina were occupied with scanty secretory material (Fig. 3a). After D-Asp i.p. injection, the glandular cells became pyramidal in shape (Fig. 3b). Numerous dilated capillaries were present in the abundant connective tissue among the acini (Fig. 3b). The glandular cells of intact rats were weakly positive for AB/PAS reaction (Fig. 3c), whereas both glandular epithelium and connective tissue of D-Asp-injected HG (at 1 h) resulted strongly positive (Fig. 3d). The glandular epithelium of 1 h D-Asp-treated HG (Fig. 3f) revealed larger and more numerous Sudan black-positive vacuoles and porphyrin accretions than did control (Fig. 3e). Two hours after D-Asp administration, coalescence of the acini, as well as

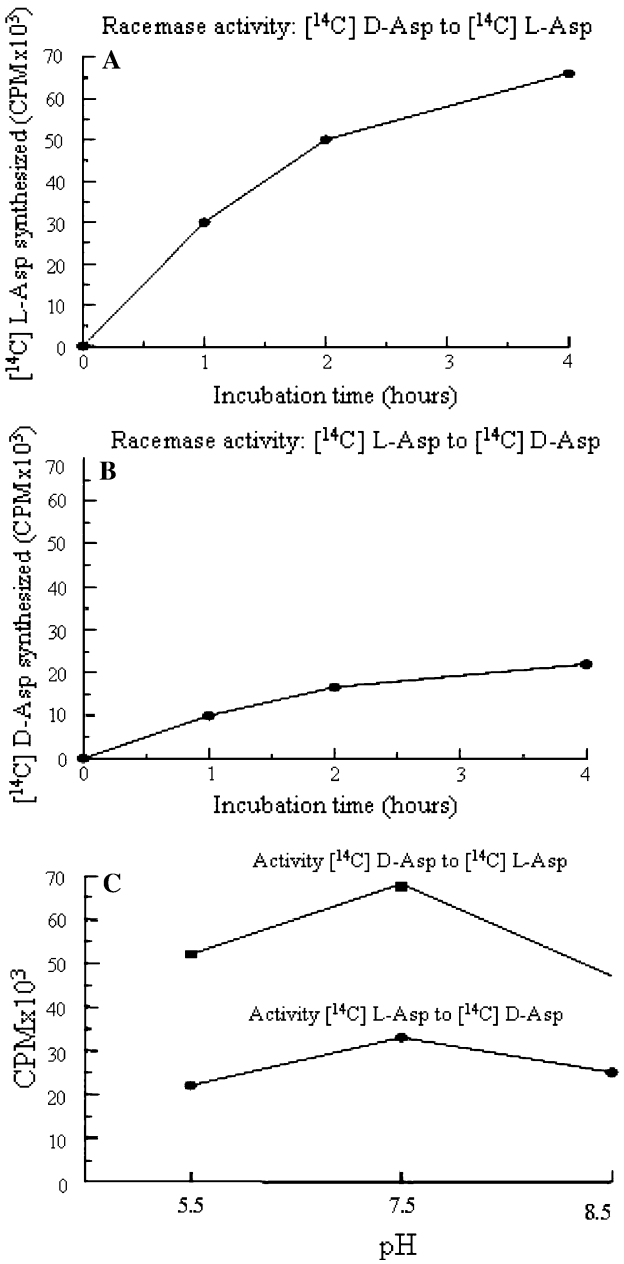

Fig. 2 Racemase activities in rat Harderian gland by in vitro study. **a** In rat, HG conversion of [^{14}C]D- to [^{14}C]L-Asp increased up until 4 h incubation. **b** Lower rates of D-Asp synthesis were observed using [^{14}C]L-Asp as precursor. **c** Racemase activities converting [^{14}C]L- to [^{14}C]D-Asp and [^{14}C]D- to [^{14}C]L-Asp at various pH; both racemase activities displayed the maximum activity at pH 7.5

holocrine secretion, could be observed (not shown). No histochemical differences were observed between control and HG, 6 h after D-Asp injections (data not shown).

Mercury bromophenol blue reaction for histochemical protein detection did not reveal differences between D-Asp-injected-HG (at all times) and control (data not shown).

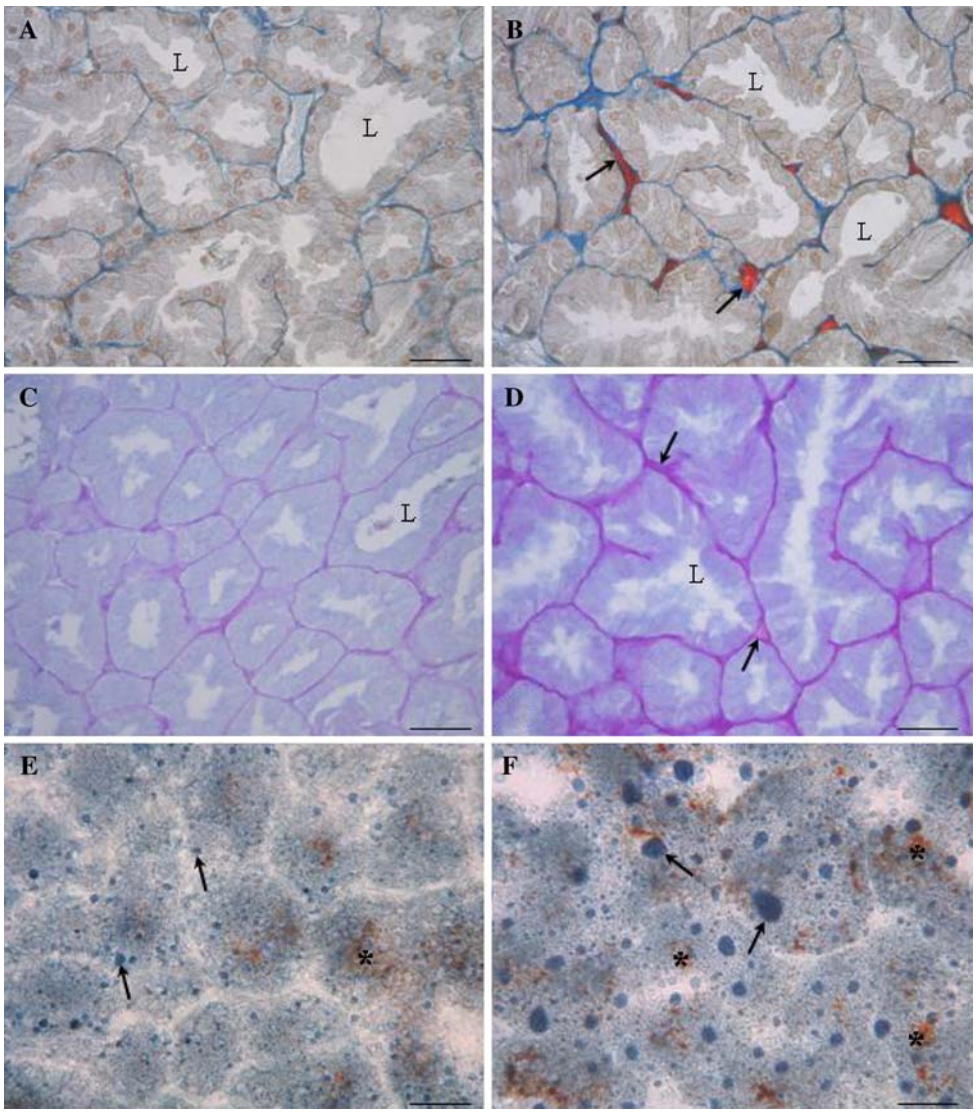

Fig. 3 Paraffin and cryostat sections of rat Harderian glands. **a** The glandular cells of control animals show basal nuclei and weakly basophilic granules in the cytoplasm, Mallory stain. **b** At 1 h after D-Asp treatment, glandular cells appear pyramidal in shape; numerous dilated capillaries are present among the acini (*arrows*), Mallory stain. **c** Glandular cells of intact rat HG are weakly positive for Alcian blue/PAS (AB/PAS). d At 1 h after D-Asp injection, both glandular epithelium and inter-acinar connective tissue (*arrows*) are strongly positive for AB/PAS. **e** Cryostat section from control rat HG. Numerous Sudan Black-positive vacuoles (*arrows*) and porphyrins accretions (*asterisk*) are present in glandular cells. **f** Cryostat section from D-Asp treated rat HG. At 1 h after D-Asp injection, large vacuoles stained with Sudan Black (*arrows*) are observed within and outside the acini. Note the numerous porphyrins accretions (*asterisks*). *L* Lumen. *Scale bars* 25 μm

Ultrastructure

As widely reported in literature, two cell types are present in rat HG (see for review Payne 1994; Chieffi et al. 1996). Type A cells have numerous large secretory vacuoles and type B cells have a few minute droplets (Fig. 4a). In both the cell types, the basally located nuclei were mostly euchromatic (Fig. 4a). In D-Asp-treated rat HG (30 min and 2 h after D-Asp injection), the glandular epithelium appeared to be constituted only by type A cells, as shown by the cytoplasm filled with large electron-lucent vacuoles (Fig. 4b); B type cells were not observed. Nuclei were mostly heterochromatic and very often showed an irregular profile (Fig. 4b). In D-Asp-treated rat HG, glandular lumina were filled with lipid droplets, nuclei and cytoplasm debris (Fig. 5a). The connective tissue among the acini was more abundant in D-Asp-treated HG than in control. Interestingly, electron micrographs revealed lipid vacuoles along intertubular strands of connective tissue in D-Asp treated-HG (Fig. 5b). Collagen fibrils contoured the vesicles and the cells.

Porphyrin levels

Fluorometric assays revealed higher levels of porphyrin in HG 30 min and 2 h after D-Asp injection (146.2 ± 3.0 μg/g tissue; 187.8 ± 3.2 μg/g tissue, respectively), as compared to control (133.5 ± 3.0 μg/g tissue).

NMDA receptor-mRNA in the rat HG

Levels of mRNA expression of the NMDA receptor subunits (NR1–NR2A–NR2B–NR2C–NR2D) in the rat HG were measured by RT-PCR. In rat HG, we found expression of NR1–NR2A–NR2B–NR2D receptor subunits (Fig. 6).

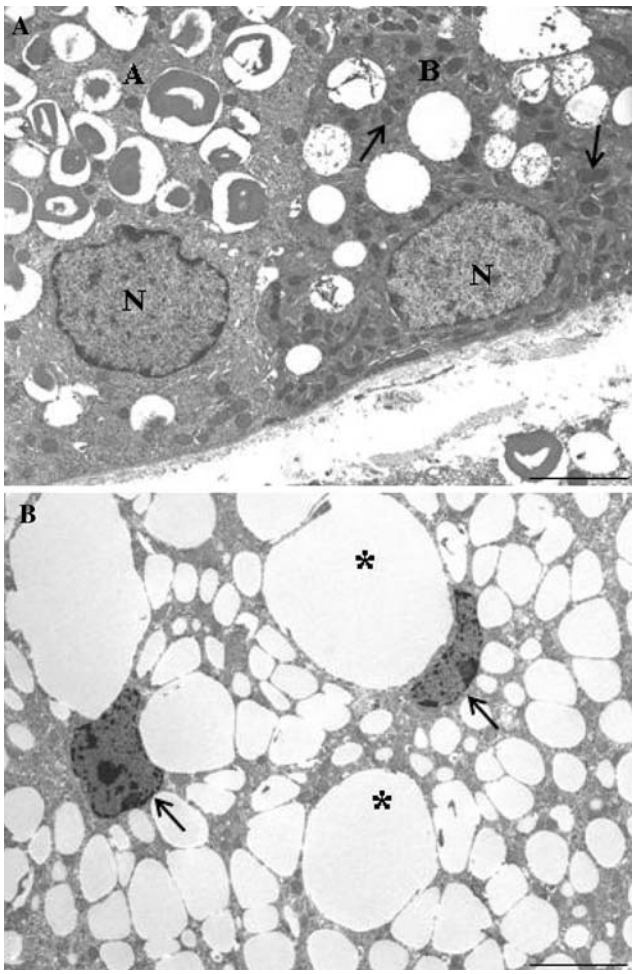

Fig. 4 Electron micrographs of rat Harderian glands. **a** HG from intact rat shows type A and type B cells. The type A cell (**a**) displays large cytoplasmic vacuoles filled with moderately electron-dense material. Type B cell (**b**) displays unstained vacuoles containing granular osmiophilic material and numerous mitochondria (*arrows*); in both cell types, the nuclei are basally located. *N* Nucleus. **b** At 1 h after D-Asp injection, glandular cells show heterochromatic nuclei (*arrows*) and the cytoplasm filled with large electron-lucent cytoplasmic vacuoles (*asterisks*). *Scale bars* 5 μm

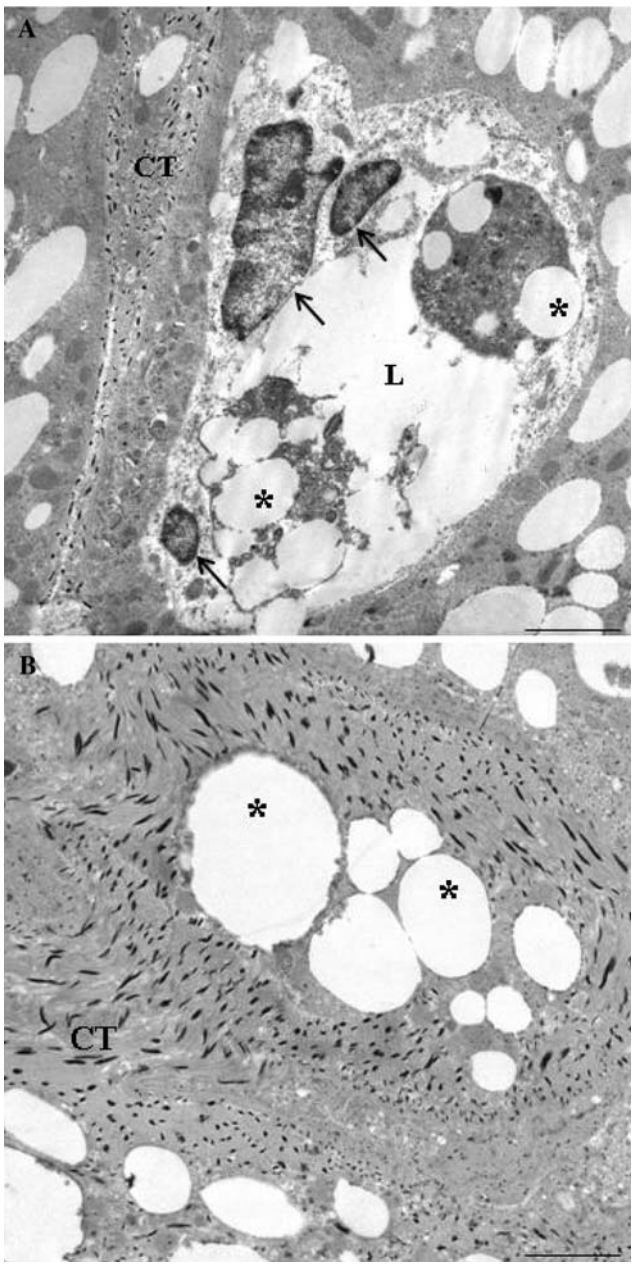

Fig. 5 Electron micrographs of rat Harderian glands at 2 h after D-Asp injection. **a** The figure shows an acinar lumen filled with nuclei (*arrows*), and cytoplasmic debris containing lipid vacuoles (*asterisks*). **b** Numerous lipid vacuoles (*asterisks*) inside inter-acinar connective tissue (*CT*) can be seen. *L* Lumen. *Scale bars* 2.5 μm

ERK1/2, JNK activities

Total proteins isolated from rat HG and liver were analyzed by Western blot analysis (Fig. 7). Expression of ERK1 (extracellular signal-regulated protein kinase) protein was higher than ERK2 protein in HG of control rats (Fig. 7). D-Asp i.p. injections did not alter the expression of ERK1 and ERK2, which indeed appeared to be equally expressed in control rats and at all time points after D-Asp injection (Fig. 7). It is important to note that the basal level of ERK1 and ERK2 activity (phosphorylation of the Thr202/Tyr204 residues) was very low in control rat HG. By contrast, after D-Asp injection, we observed an increase in the activity of both ERK1 and ERK2 at both 30 min and 2 h (ERK1:

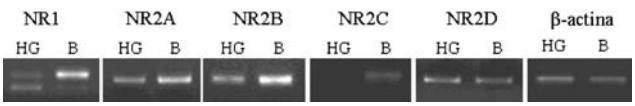

Fig. 6 RT-PCR-based measurement of NMDA receptor subunit (NR1–NR2A–NR2B–NR2C–NR2D) mRNA levels in both rat Harderian gland and brain (**b**). *β*-Actin mRNA levels were measured as the internal standard. Each *lane* contains PCR product derived from the appropriate cDNA, for which 2 μg of total RNA was used

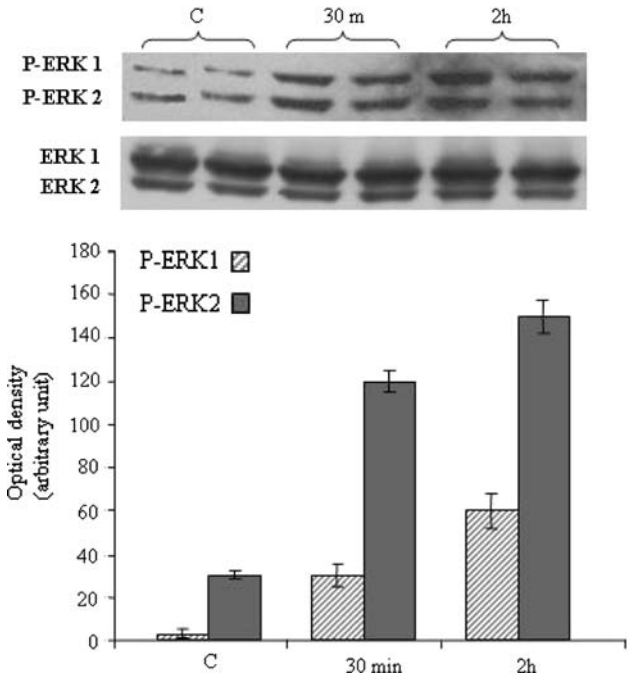

Fig. 7 Western blot detection of ERK1/2 proteins in rat Harderian gland in control (*C*) and at 30 min and 2 h after D-Asp injection. Two pools of HGs (each from three animals) were stained for either ERK1/2 or *P-ERK1/2*. Specific bands of 44 kDa for ERK1 and 42 kDa for ERK2 were observed by comparison with co-migrating size markers (Bio-Rad, Melville, NY). The amount of activated ERK1/2 was quantified using the scan program and normalized with respect to total ERK1/2

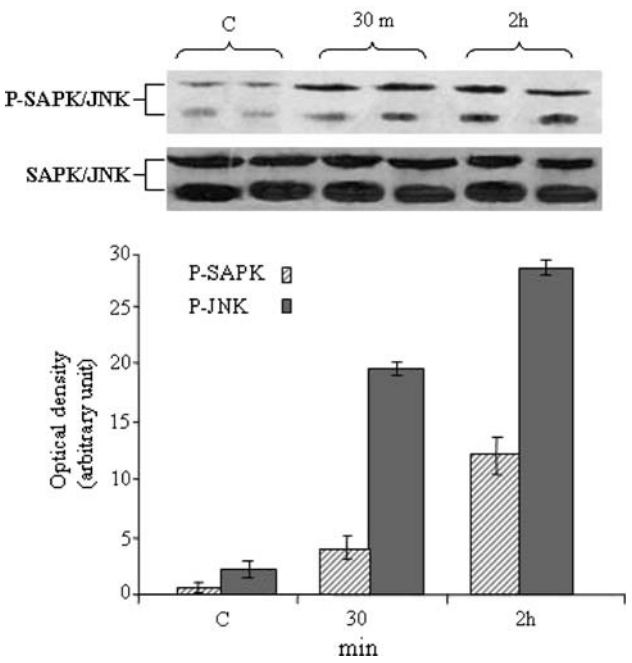

Fig. 8 Western blot detection of SAPK/JNK proteins in rat Harderian gland in control (*C*) and 30 min and 2 h after D-Asp injection. Two pools of HGs (each from three animals) were stained for either SAPK/JNK or *P-SAPK/JNK*. Specific bands of 54 and 46 kDa were observed by comparison with co-migrating size markers (Bio-Rad, Melville, NY). The amount of activated SAPK/JNK was quantified using the scan program and normalized with respect to total SAPK/JNK

about 10- and 20-fold, respectively, vs. control; ERK2: about four- and fivefold, respectively, vs. control). Similarly, D-Asp treatment did not significantly alter the expression of SAPK/JNK (stress-activated protein kinase/c-jun N-terminal kinase) itself, which appeared to be equally expressed in control rats and at all time points after D-Asp injection (Fig. 8). However, the treated HG did display a slight increase in SAPK/JNK activity (phosphorylation of the Thr183/Tyr185 residues) at both 30 min and 2 h with respect to basal levels (about 9- and 13-fold, respectively, vs. control) (Fig. 8).

In the liver, ERK1/2 and SAPK/JNK activation remained unaltered at all times after D-Asp injection (data not shown).

NOS activity, cAMP, and cGMP levels

Nitric oxide synthase (NOS) activity was measured by the colorimetric method. D-Asp injection induced a rapid (at 15 min) and substantial increase in NOS activity in rat HG. However, 45 min and 1 h after D-Asp injection, NOS activity was close to control values (time 0) (Table 1). A significant increase in cGMP concentration was observed in rat HG up to 1 h after D-Asp injection, as compared to time 0 (Table 1).

An increase in cAMP concentration was also observed in the rat HG 15 min, 45 min, and 1 h after D-Asp i.p. injection with respect to control (time 0) (Table 1).

No differences either in NOS activity, in cGMP, or in cAMP concentrations were detected between control liver and D-Asp-injected liver (at all times) (Table 1).

Discussion

In accordance with our previous studies demonstrating the occurrence of high levels of D-Aspartate in the Harderian glands of vertebrate species (Raucci et al. 2005; Santillo et al. 2006), we report here the presence of significant amounts of free D-Asp in the Harderian gland of adult male rats. Remarkably, we demonstrated that rat HG possesses the capability to uptake and accumulate exogenously administered D-Asp, with the greatest D-Asp accumulation occurring at 6 h after its administration (Fig.1). Interestingly, as demonstrated by our experiments in vitro, D-Asp was in part converted to L-Asp by virtue of an aspartate racemase that converts D-Asp to L-Asp in rat HG (Fig. 2a). Accordingly, we deduced that this enzyme could play an essential role in decreasing excessive amounts of D-Asp in the tissues, a phenomenon that, if left unchecked, could

Table 1 Effects of D-aspartate injection on the NOS activity and on the cAMP and cGMP levels in rat Harderian gland and liver

Time after D-Asp injection	Nitrite + nitrate (μM)		cGMP (pmol/g tissue)		cAMP (pmol/g tissue)	
	HG	L	HG	L	HG	L
Time 0	28.3 ± 8.4	16.3 ± 7.1	50 ± 6	93 ± 9	401 ± 52	410 ± 33
15 min	59.5 ± 7.3*	16.2 ± 6.3	214 ± 32*	82 ± 6	807 ± 58*	350 ± 31
45 min	36.6 ± 1.4	22.0 ± 5.2	400 ± 41*	91 ± 6	2500 ± 89**	393 ± 24
1 h	23.9 ± 5.2	19.1 ± 7.4	321 ± 23*	89 ± 8	921 ± 51*	406 ± 46

The results represent the mean ± SD obtained from five individual determinations

HG Harderian gland, *L* liver

* $P < 0.001$

** $P < 0.0001$ vs. control

have detrimental effects on the animal (D'Aniello et al. 1993). Furthermore, we also found that the racemase activity converting L-Asp to D-Asp (Fig. 2b) was lower than the aspartate racemase converting D-Asp to L-Asp. Thus, we hypothesized that free D-Asp in the HG was elicited by the activity of this enzyme. Consistently, a D-Asp racemase enzyme that specifically converts D to L and does not act on other amino acids has been purified from bacteria (Okada et al. 1991; Yamashita et al. 2004) and mollusks (Shibata et al. 2003; D'Aniello et al. 2005; Spinelli et al. 2006). Remarkably, however, not too long ago we reported the presence of another D-Asp racemase that converts L to D in cultured rat neurons (Wolosker and et al. 2000) and in frog HG (Raucci et al. 2005). In addition to aspartate racemase, other racemases that convert other L to respective D forms have been demonstrated. For instance, Wolosker et al. (1999) have reported the presence of a serine racemase that converts L-Ser to D-Ser in rat brain. More recently, D-serine racemase has also been evidenced in the neuronal ganglion cells of rat retina (Stevens et al. 2003).

Albeit D-Asp specific receptors have not yet been identified, a number of reports indicate that NMDA receptors have an affinity for L-Glu and L-Asp, as well as for D-Asp (Skerritt and Johnston1981; Foster and Fagg 1987). In line with these studies, our RT-PCR analyses characterized the expression of NR1–NR2A–NR2B–NR2D receptor subunits in rat HG (Fig. 6).

Our present histochemical studies demonstrated that i.p. injection of D-Asp stimulates the secretory activity in the rat HG (Fig. 3). The most notable effect of D-Asp administration was the increase in lipid secretion. More specifically, the morphological study of the HG at various time points after D-Asp administration indicated that the amino acid rapidly activated a massive glandular secretion, thus invading the glandular lumina and the inter-alveolar connective tissue. Consistently, electron microscopy revealed that, in D-Asp injected HG, the glandular lumina were filled with cytoplasmic debris and nuclei, as well as lipid vacuoles inside the connective tissue (Fig. 5). Only A cell types were present in the glandular epithelium of D-Asp treated rats (Fig. 4). These cells showing, in general, heterochromatic nuclei and a cytoplasm filled with large secretory vacuoles, closely resemble the features of adipocytes. It has been proposed that A and B cells could represent the different stages of a secretory cycle, with B cells representing the initial stage and A cells the end of the activity cycle (Woodhouse and Rhodin 1963; Chieffi Baccari et al. 2004). Therefore, by promoting secretory activity, D-Asp injection might induce the conversion of B cells to A cells.

As demonstrated by the histochemical reaction for proteins, as well as by the biochemical studies (total protein and electrophoresis), D-Asp injection was unable to modify the protein content of the gland (data not shown). Although rat HGs normally secrete lipoproteic substances, our histochemical tests revealed the presence of muco-substances in the glandular cells of rat HG after D-Asp treatment (Fig. 3), suggesting that a biochemical modification of HG secretion took place. This finding is further supported by previous studies reporting a significant increase in mucous secretion in both frog (Raucci et al. 2005) and lizard HGs (Santillo et al. 2006) after D- Asp acute treatment. Interestingly, AB/PAS reaction and electron micrographs revealed a more abundant connective tissue among the glandular acini of D-Asp treated HGs with respect to control HG (Fig. 3). Such increase could be associated with the potential capability of D-Asp to stimulate the secretory activity of fibroblasts, thus contributing to an enhanced production of extracellular matrix. This remarkable and unexpected finding may lead the way to more insightful research on the mechanisms underlying such phenomenon.

Therefore, since D-Asp injection induced an enhanced glandular secretion in rat HG and since we hypothesized that the secretory activation could be mediated by NMDA receptors, we investigated the molecular pathways elicited by the activation of NMDA mediated by D-Asp. Recent

studies have reported that NMDA activation induces phosporylation of ERK (Finkbeiner and Greenberg 1996; Kornhauser and Greenberg 1997; Chandler et al. 2001). ERK belongs to the MAP kinases comprising a family of serine/threonine kinases that occupy a focal point in signal transduction, mainly by activating gene transcription via translocation into the nucleus (Zhang et al. 1995; Cobb 1999). As D-Asp injection activated ERK1/2 in rat HG (Fig. 7), we hypothesized that D-Asp mediated NMDA activation might enhance the kinase pathway. These current results reinforce our previous observations revealing an increase in ERK activity in the frog HG after D-Asp acute treatment (Raucci et al. 2005). The activity of these important regulators of cellular signaling is normally reversibly regulated by threonine–tyrosine phosphorylation (Zhang et al. 1995).

We also presented morphological evidence of a powerful hyperaemia in D-Asp-treated rat HG (Fig. 3). This same effect, due to D-Asp administration, has already been described in one of our previous studies on frog HG (Raucci et al. 2005). In rat HG, we found an increase in NOS activity 15 min after D-Asp treatment (Table 1). NOS activity is commonly measured and reflects the NO levels. Specifically, NO, a gaseous substance produced by NOS and synthesized by L-arginine (Stuehr et al. 1989), is well recognized as an endothelial-derived relaxing factor (Ignarro et al. 1987; Palmer et al. 1987). It is well known that NO diffuses in smooth muscle cells by activating a guanylyl cyclase that, in turn, produces cGMP from GTP with consequent smooth muscle relaxation and vasodilatation. We found increased levels of cGMP in rat HG up to 1 h after D-Asp injection (Table 1). Similarly, D-Asp could activate NMDA receptors which, in turn, could induce NOS activation. Consistently, Bredt and Snyder (1989, 1990) demonstrated that glutamate, by acting on NMDA receptors, triggers a rapid, substantial increase in NOS activity by permeating Ca^{2+} ions.

On the other hand, NOS is also phosphorylated by multiple kinases including cAMP-dependent protein kinase (Zhang and Hintze 2006; Busch and Borda 2007). Consistent with previous studies indicating that D-Asp injection into live animals or added to incubation media of cultured neurons triggers an increase in cAMP (Spinelli et al. 2006), we found that increased levels of cAMP occurred up to 1 h after D-Asp injection (Table 1).

A noteworthy feature of rat HG is the very high porphyrinogenic activity (Gorchein2003; Yang et al. 2006). In our study we found that 2 h after D-Asp injection, porphyrin secretion increased by about 30% with respect to basal levels. It has been shown that porphyrin accumulation can result in cell damage, owing to the ability of porphyrins to produce reactive oxygen species (ROS) when exposed to light (Reiter and Klein 1971; Coto-Montes et al. 2001; Hardeland et al. 2003; Tomás-Zapico et al. 2003, 2005). Hence, because studies of cultured hepatocyte and rodent models of oxidative stress have demonstrated that JNK promotes cell death (Czaja 2007), we hypothesized that the increase in ROS induced by D-Asp administration in the HG could induce the activation of JNK pro-apoptotic pathways, an event most likely promoted by the gland to hinder cellular damage.

Interestingly, although high D-Asp exogenous concentrations did accumulate in the liver, ERK1/2, JNK, and NO pathways were not activated. Similarly, no increases in cAMP and cGMP levels were observed (Table 1). Thus, we deduced that the effects of D-Asp on rat HG were specific only to this gland.

In conclusion, physiological role of D-Asp rat HG was corroborated by the presence of high concentrations of free D-Asp and by the racemase activity observed in the gland. In particular, our experimental data indicate that D-Asp acute treatment dramatically enhances lipid and porphyrin secretion in the gland and induces a powerful hyperaemia in inter-acinar interstitial tissue. Since D-Asp is recognized by NMDA receptors and the expression of such receptors was found in rat HG, we hypothesized that D-Asp induces the activation of ERK and NOS pathways mediated by NMDA. Interestingly, as a result of enhanced oxidative stress due to increased porphyrin secretion, we deduced that the activation of SAPK/JNK pro-apoptotic pathway could be triggered by the gland to maintain its cellular integrity. Most importantly, we demonstrated that D-Asp injection induces hypertrophy of the interstitial compartment, a novel finding that may lead the way to more insightful research on the mechanisms of such phenomenon. Therefore, this study adds substantial support to the theory that D-Asp plays a prominent physiological role in eliciting exocrine secretion.

Acknowledgments We thank Mr. Franco Iamunno for technical assistance with electron microscopy and Dr. Paola Merolla for English editorial assistance.

References

Bredt DS, Snyder SH (1989) Nitric oxide mediates glutamate-linked enhancement of cGMP levels in the cerebellum. Proc Natl Acad Sci USA 86:9030–9033

Bredt DS, Snyder SH (1990) Isolation of nitric oxide synthetase, a calmodulin-requiring enzyme. Proc Natl Acad Sci USA 87:682–685

Busch L, Borda E (2007) Signaling pathways involved in pilocarpine-induced mucin secretion in rat submandibular glands. Life Sci 80:842–851

Buzzell GR, Menendez-Pelaez A, Porkka-Heiskanen T, Pangerl A, Pangerl B, Vaughan MK, Reiter RJ (1989) Bromocriptine prevents the castration-induced rise in porphyrin concentration in the harderian glands of the male Syrian hamster, *Mesocricetus auratus*. J Exp Zool 249:172–176

Chandler LJ, Sutton G, Dorairaj NR, Norwood D (2001) *N*-methyl D-aspartate receptor-mediated bidirectional control of extracellular signal-regulated kinase activity in cortical neuronal cultures. J Biol Chem 276:2627–2636

Chieffi Baccari G, Monteforte R, de Lange P, Rauchi F, Farina P, Lanni A (2004) Thyroid hormone affects secretory activity and uncoupling protein-3 expression in rat harderian gland. Endocrinology 145:3338–3345

Chieffi G, Chieffi Baccari G, Di Matteo L, d'Istria M, Minucci S, Varriale B (1996) Cell biology of harderian gland. Int Rev Cytol 168:1–80

Cobb MH (1999) MAP kinase pathways. Prog Biophys Mol Biol 71:479–500

Coto-Montes A, Boga JA, Tomás-Zapico C, Rodríguez-Colunga MJ, Martínez-Fraga J, Tolivia-Cadrecha D, Menéndez G, Hardeland R, Tolivia D (2001) Physiological oxidative stress model: Syrian hamster Harderian gland-sex differences in antioxidant enzymes. Free Radic Biol Med 30:785–792

Coto-Montes A, Tomás-Zapico C, Escames G, León J, Rodríguez-Colunga MJ, Tolivia D, Acuña-Castroviejo D (2003) Specific binding of melatonin to purified cell nuclei from mammary gland of swiss mice: day-night variations and effect of continuous light. J Pineal Res 34:297–301

Czaja MJ (2007) Cell signaling in oxidative stress-induced liver injury. Semin Liver Dis 27:378–389

D'Aniello A (2007) D-Aspartic acid: an endogenous amino acid with an important neuroendocrine role. Brain Res Rev 53:215–234

D'Aniello A, D'Onofrio G, Pischetola M, D'Aniello G, Vetere A, Petrucelli L, Fisher GH (1993) Biological role of D-amino acid oxidase and D-aspartate oxidase. Effects of D-amino acids. J Biol Chem 268:26941–26949

D'Aniello A, Di Fiore MM, Fisher GH, Milone A, Seleni A, D'Aniello S, Perna AF, Ingrosso D (2000a) Occurrence of D-aspartic acid and *N*-methyl-D-aspartic acid in rat neuroendocrine tissues and their role in the modulation of luteinizing hormone and growth hormone release. FASEB J 14:699–714

D'Aniello G, Tolino A, D'Aniello A, Errico F, Fisher GH, Di Fiore MM (2000b) The role of D-aspartic acid and *N*-methyl-D-aspartic acid in the regulation of prolactin release. Endocrinology 141:3862–3870

D'Aniello A, Spinelli P, De Simone A, D'Aniello S, Branno M, Aniello F, Fisher GH, Di Fiore MM, Rastogi RK (2003) Occurrence and neuroendocrine role of D-aspartic acid and *N*-methyl-D aspartic acid in *Ciona intestinalis*. FEBS Lett 552:193–198

D'Aniello S, Spinelli P, Ferrandino G, Peterson K, Tsesarskia M, Fisher G, D'Aniello A (2005) Cephalopod vision involves dicarboxylic amino acids: D-aspartate, L-aspartate and L-glutamate. Biochem J 386:331–340

Djeridane Y, Vivien-Roels B, Simonneaux V, Miguez JM, Pevet P (1998) Evidence for melatonin synthesis in rodent Harderian gland: a dynamic in vitro study. J Pineal Res 25:54–64

Djeridane Y, Klosen P, Vivien-Roels B, Simonneaux V, Pévet P (1999) Immunohistochemical evidence for the presence of tryptophan hydroxylase and serotonin in the rodent Harderian gland. Cell Tissue Res 296:517–523

Dunlop DS, Neidle A, McHale D, Dunlop DM, Lajtha A (1986) The presence of free D-aspartic acid in rodents and man. Biochem Biophys Res Commun 26:27–32

Finkbeiner S, Greenberg ME (1996) Ca^{2+}-dependent routes to Ras: mechanisms for neuronal survival, differentiation, and plasticity? Neuron 16:233–236

Foster AC, Fagg GE (1987) Comparison of L-[^{3}H]glutamate, D-[^{3}H]aspartate, DL-[^{3}H]AP5 and [^{3}H]NMDA as ligand for NMDA receptors in crude postsynaptic densities from rat brain. Eur J Pharmacol 133:291–300

Gorchein A (2003) Characterization of porphyrins of rat Harderian gland by thin layer chromatography and mass spectrometry: no evidence for a tricarboxylic acid porphyrin. Biomed Chromatogr 17:526–529

Hardeland R, Coto-Montes A, Poeggeler B (2003) Circadian rhythms, oxidative stress, and antioxidative defense mechanisms. Chronobiol Int 20:921–962

Hoffman RA, Johnson LB, Reiter RJ (1989) Regulation of melatonin in the harderian glands of golden hamsters. J Pineal Res 6:63–71

Hugo J, Krijt J, Vokurka M, Janousek V (1987) Secretory response to light in rat Harderian gland: possible photoprotective role of Harderian porphyrin. Gen Physiol Biophys 6:401–404

Ignarro LJ, Buga GM, Wood KS, Byrns RE, Chaudhuri G (1987) Endothelium-derived relaxing factor produced and released from artery and vein is nitric oxide. Proc Natl Acad Sci USA 84:9265–9269

Kornhauser JM, Greenberg ME (1997) A kinase to remember: dual roles for MAP kinase in long-term memory. Neuron 18:839–842

Masuda W, Nouso C, Kitamura C, Terashita M, Noguchi T (2003) Free D-aspartic acid in rat salivary glands. Arch Biochem Biophys 420:46–54

Nagata Y, Homma H, Matsumoto M, Imai K (1999) Stimulation of steroidogenic acute regulatory protein (StAR) gene expression by D-aspartate in rat Leydig cells. FEBS Lett 454:317–320

Nahm WK, Philpot BD, Adams MM, Badiavas EV, Zhou LH, Butmarc J, Bear MF, Falanga V (2004) Significance of *N*-methyl-D-aspartate (NMDA) receptor-mediated signaling in human keratinocytes. J Cell Physiol 200:309–317

Neidle A, Dunlop DS (1990) Developmental changes in free D-aspartic acid in the chicken embryo and in the neonatal rat. Life Sci 46:1517–1522

Okada H, Yohda M, Giga-Hama Y, Ueno Y, Ohdo S, Kumagai H (1991) Distribution and purification of aspartate racemase in lactic acid bacteria. Biochem Biophys Acta 1078:377–382

Palmer RM, Ferrige AG, Moncada S (1987) Nitric oxide release accounts for the biological activity of endothelium-derived relaxing factor. Nature 327:524–526

Payne AP (1994) The harderian gland: a tercentennial review. J Anat 185:1–49

Raucci F, Santillo A, D'Aniello A, Chieffi P, Chieffi Baccari G (2005) D-Aspartate modulates transcriptional activity in Harderian gland of frog, *Rana esculenta*: morphological and molecular evidence. J Cell Physiol 204:445–454

Reiter RJ, Klein DC (1971) Observations on the pineal gland, the Harderian glands, the retina, and the reproductive organs of adult female rats exposed to continuous light. J Endocrinol 51:117–125

Santillo A, Monteforte R, Raucci F, D'Aniello A, Chieffi Baccari G (2006) Occurrence of D-aspartate in the Harderian gland of *Podarcis s. sicula* and its effect on gland secretion. J Exp Zool 305:610–619

Schell MJ, Cooper OB, Snyder SH (1997) D-aspartate localizations imply neuronal and neuroendocrine roles. Proc Natl Acad Sci USA 94:2013–2018

Seyama Y, Kasama T, Yasugi E, Park SH, Kano K (1992) Lipids in Harderian glands and their significance. In: Webb SM, Hoffman RA, Puig-Domingo ML, Reiter RJ (eds) Harderian glands: porphyrin metabolism, behavior and endocrine effects. Springer, Berlin

Shanas U, Terkel J (1996) Grooming secretions and seasonal adaptations in the blind mole rat (*Spalax ehrenbergi*). Physiol Behav 60:653–656

Shibata K, Watanabe T, Yoshikawa H, Abe K, Takahashi S, Kera Y, Yamada RH (2003) Purification and characterization of aspartate racemase from the bivalve mollusk *Scapharca broughtonii*. Comp Biochem Physiol B Biochem Mol Biol 134:307–314

Skerritt JH, Johnston GA (1981) Uptake and release of *N*-methyl-D-aspartate by rat brain slices. J Neurochem 36:881–885

Spinelli P, Brown E, Ferrandino G, Branno M, Montarolo PG, D'Aniello E, Rastogi RK, D'Aniello B, Baccari G, Fisher G, D'Aniello A (2006) D-Aspartic acid in the nervous system of *Aplysia limacina*: possible role in neurotransmission. J Cell Physiol 206:672–681

Stevens ER, Esguerra M, Kim PM, Newman EA, Snyder SH, Zahs KR, Miller RF (2003) D-Serine and serine racemase are present in the vertebrate retina and contribute to the physiological activation of NMDA receptors. Proc Natl Acad Sci USA 100:6789–6794

Stuehr DJ, Kwon NS, Gross SS, Thiel BA, Levi R, Nathan CF (1989) Synthesis of nitrogen oxides from L-arginine by macrophage cytosol: requirement for inducible and constitutive components. Biochem Biophys Res Commun 161:420–426

Thiessen DD (1988) Body temperature and grooming in the Mongolian gerbil. Ann NY Acad Sci 525:27–39

Tomás-Zapico C, Coto-Montes A, Martínez-Fraga J, Rodríguez-Colunga MJ, Tolivia D (2003) Effects of continuous light exposure on antioxidant enzymes, porphyric enzymes and cellular damage in the Harderian gland of the Syrian hamster. J Pineal Res 34:60–68

Tomàs-Zapico C, Caballero B, Sierra V, Vega-Naredo I, Alvarez-Garcia O, Tolivia D, Rodriguez-Colunga MJ, Coto-Montes A (2005) Survival mechanisms in a physiological oxidative stress model. FASEB J 19:2066–2068

Wang H, Wolosker H, Pevsner J, Snyder SH, Selkoe DJ (2000) Regulation of rat magnocellular neurosecretory system by D aspartate: evidence for biological role(s) of a naturally occurring free D-amino acid in mammals. J Endocrinol 167:247–252

Wolosker H, Sheth KN, Takahashi M, Mothet JP, ROJr Brady, Ferris CD, Snyder SH (1999) Purification of serine racemase: biosynthesis of the neuromodulator D-serine. Proc Natl Acad Sci USA 96:721–725

Wolosker H, D'Aniello A, Snyder SH (2000) D-Aspartate disposition in neuronal and endocrine tissues: ontogeny, biosynthesis and release. Neuroscience 100:183–189

Woodhouse MA, Rhodin JAG (1963) The ultrastructure of the Harderian gland of the mouse with particular reference to the formation of its secretory product. J Ultrastruct Res 9:76–98

Yamashita T, Ashiuchi M, Ohnishi K, Kato S, Nagata S, Misono H (2004) Molecular identification of monomeric aspartate racemase from *Bifidobacterium bifidum*. Eur J Biochem 271:4798–4803

Yang JW, Afjehi-Sadat L, Gelpi E, Kunze M, Höger H, Fleckner J, Berger J, Lubec G (2006) Proteome profiling in the rat Harderian gland. J Proteome Res 5:1751–1762

Zhang XP, Hintze TH (2006) cAMP signal transduction induces eNOS activation by promoting PKB phosphorylation. Am J Physiol Heart Circ Physiol 290:2376–2384

Zhang W, Dziak RM, Aletta JM (1995) EGF-mediated phosphorylation of extracellular signal regulated kinases in osteoblastic cells. J Cell Physiol 162:348–358